

Copyright WILEY-VCH Verlag GmbH & Co. KGaA, 69469 Weinheim, Germany, 2015.

# ADVANCED ENERGY MATERIALS

Supporting Information

for *Adv. Energy Mater.*, DOI: 10.1002/aenm.201800379

## **On the Balance of Intercalation and Conversion Reactions in Battery Cathodes**

*Daniel C. Hannah, Gopalakrishnan Sai Gautam, Pieremanuele Canepa, and Gerbrand Ceder\**

DOI: 10.1002/aenm.201800379

**Article type: Full paper (Supporting information)**

**–Supporting information for–**

**On the Balance of Intercalation and Conversion Reactions in Battery Cathodes**

*Daniel C. Hannah, Gopalakrishnan Sai Gautam, Pieremanuele Canepa and Gerbrand Ceder\**

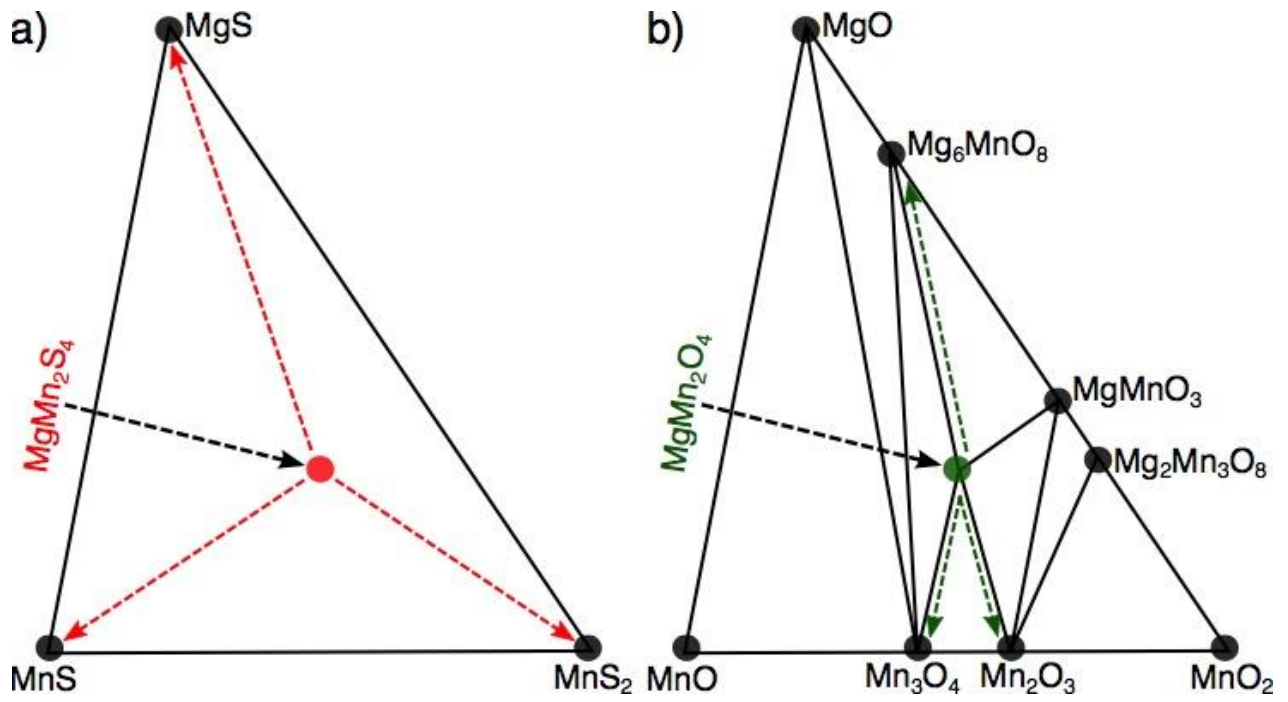
Dr. Daniel C. Hannah, Dr. Gopalakrishnan Sai Gautam, Dr. Pieremanuele Canepa and Prof. Gerbrand Ceder  
Materials Science Division, Lawrence Berkeley National Laboratory, Berkeley CA 94720, USA

Dr. Gopalakrishnan Sai Gautam  
Department of Materials Science and Engineering, Massachusetts Institute of Technology, Cambridge MA 02139, USA  
Present address: Department of Mechanical and Aerospace Engineering, Princeton University, Princeton NJ 08544, USA

Dr. Gopalakrishnan Sai Gautam and Prof. Gerbrand Ceder  
Department of Materials Science and Engineering, University of California Berkeley, CA 94720, USA

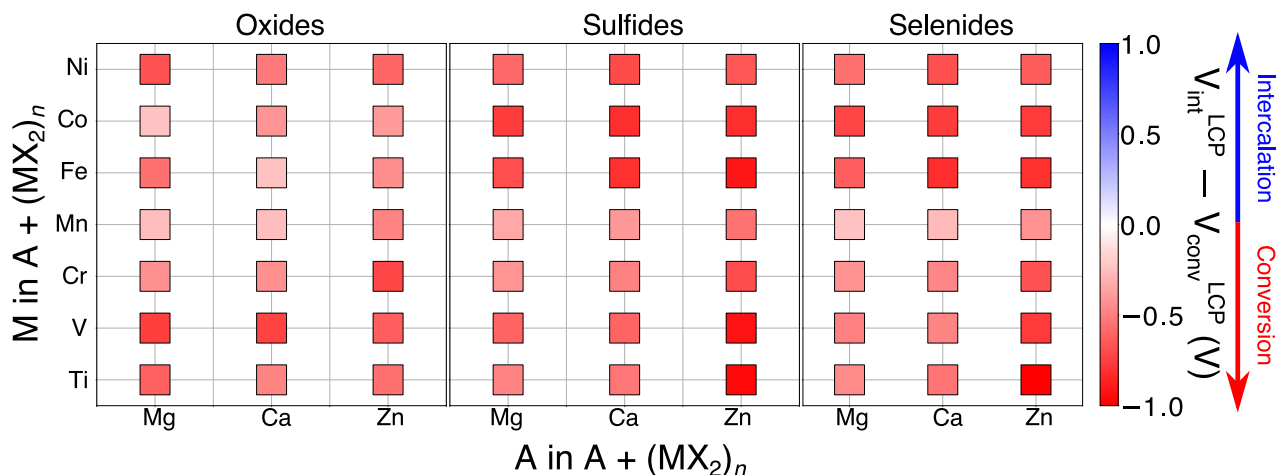
Dr. Daniel C. Hannah and Dr. Gopalakrishnan Sai Gautam  
Equally contributed to the work

S1. Ternary phase diagram for the Mg-Mn-X (X = O, S) system



**Figure S1:** (Color online) Ternary phase diagram for the (a) Mg-Mn-S and (b) Mg-Mn-O systems generated from the Materials Project database. Note that the phase diagrams display only the chemical space of relevance for intercalation or conversion reactions and are hence bound by  $\text{MgX}$ ,  $\text{MnX}$  and  $\text{MnX}_2$  compounds. Thermodynamically stable phases on the borders of the phase diagram are shown as black circles and their corresponding compositions are labeled. Solid black lines indicate tie-lines connecting stable compounds.  $\text{MgMn}_2\text{S}_4$  (panel a), the product of a one-electron intercalation reaction between Mg and  $\text{MnS}_2$ , is thermodynamically unstable ( $E^{\text{hull}}=61$  meV/atom) and shown as a red circle, while  $\text{MgMn}_2\text{O}_4$  (panel b), the product of a one-electron intercalation reaction between Mg and  $\text{MnO}_2$ , is thermodynamically stable ( $E^{\text{hull}}=0$  meV/atom) and is shown as a green circle. Dashed red arrows in panel a indicate the conversion products ( $\text{MgS}$ ,  $\text{MnS}$  and  $\text{MnS}_2$ ) that form spontaneously when Mg reduces  $\text{MnS}_2$ . Dashed green arrows in panel b indicate the conversion products ( $\text{Mg}_6\text{MnO}_8$ ,  $\text{Mn}_3\text{O}_4$  and  $\text{Mn}_2\text{O}_3$ ) that will form if Mg reduction of  $\text{MnO}_2$  does not lead to the intercalation product, spinel- $\text{MgMn}_2\text{O}_4$ . Thermodynamically unstable phases (with the exception of  $\text{MgMn}_2\text{S}_4$ ) are not shown in both panels.

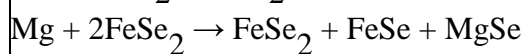
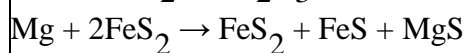
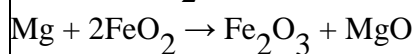
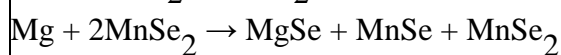
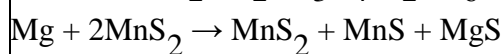
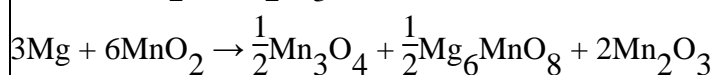
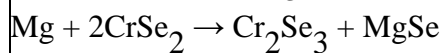
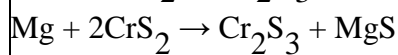
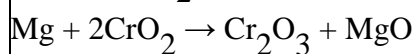
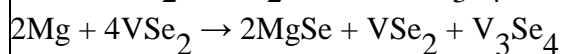
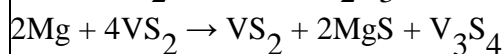
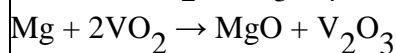
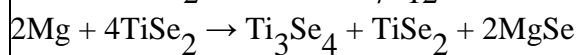
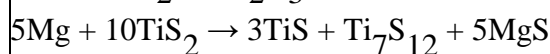
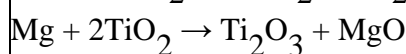
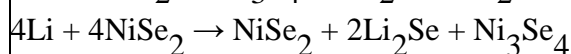
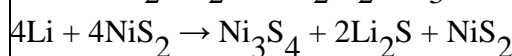
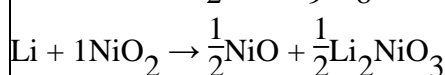
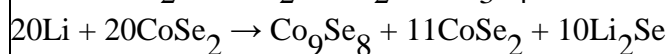
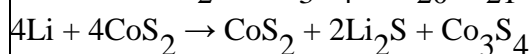
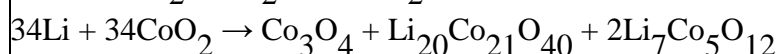
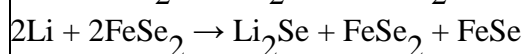
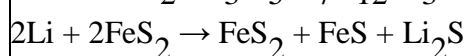
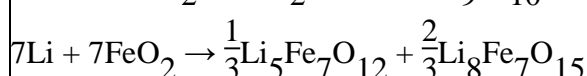
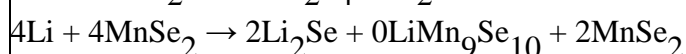
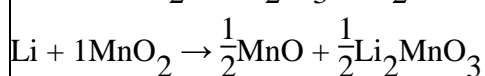
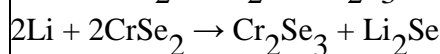
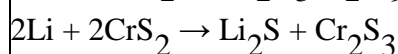
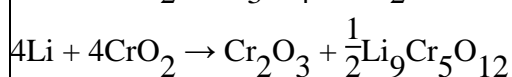
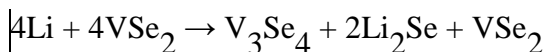
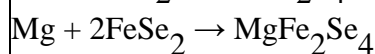
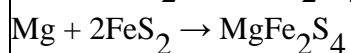
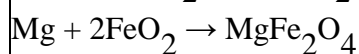
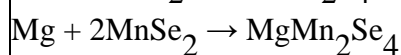
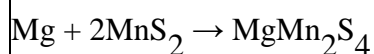
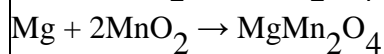
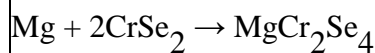
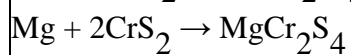
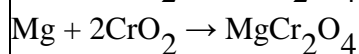
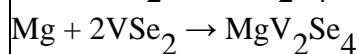
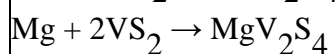
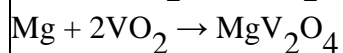
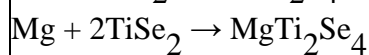
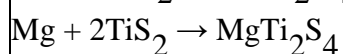
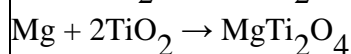
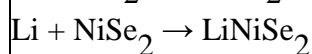
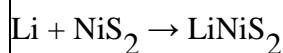
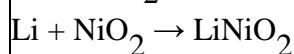
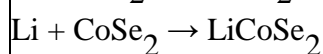
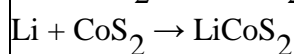
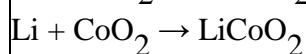
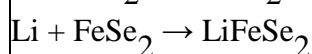
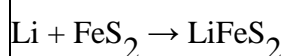
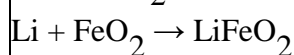
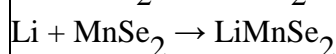
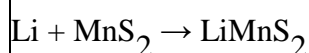
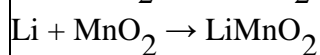
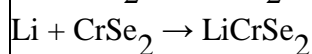
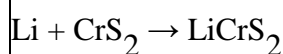
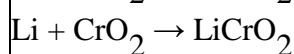
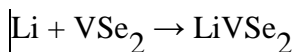
## S2. Two-electron Reduction: LCP voltages

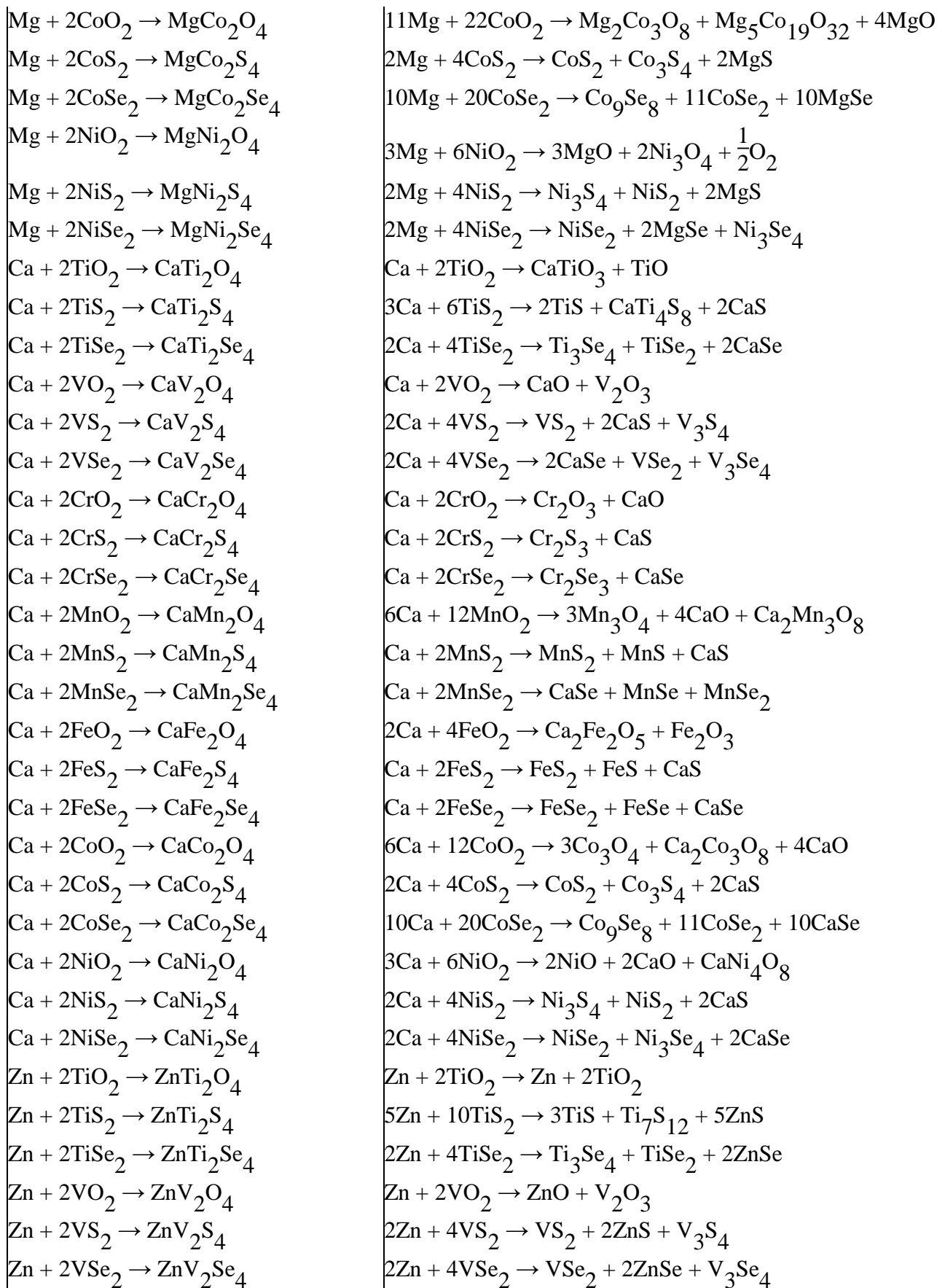


**Figure S2:** Difference between the intercalation ( $V_{\text{int}}^{\text{LCP}}$ ) and conversion ( $V_{\text{conv}}^{\text{LCP}}$ ) voltage for 2-electron reduction reactions, starting from the lowest energy charged polymorph (LCP). The voltage difference is indicated for three working ions ( $A = \text{Mg}$ ,  $\text{Ca}$ , and  $\text{Zn}$ ) in various 3d-transition metal oxide, sulfide, and selenide hosts. Higher intercalation voltages are indicated by blue-colored squares while higher conversion voltages are red-colored. The intercalation of divalent ions considered is into a  $\text{MX}_2$  structure, corresponding to a  $2e^-$  (per transition metal ion) reduction.

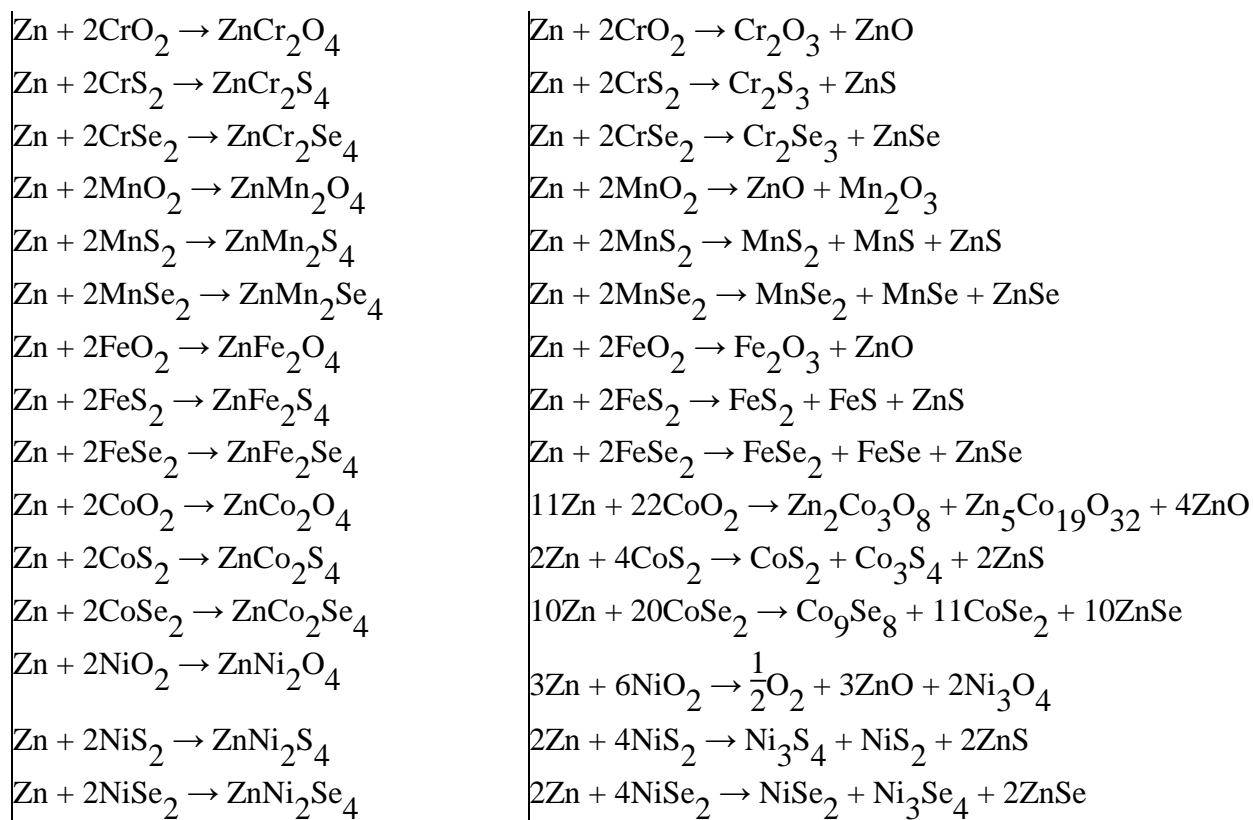
## S3. One-electron reactions considered in this work

Intercalation Reaction	Conversion Reaction
$\text{Na} + \text{TiO}_2 \rightarrow \text{NaTiO}_2$	$8\text{Na} + 8\text{TiO}_2 \rightarrow \text{Na}_8\text{Ti}_5\text{O}_{14} + \text{TiO} + \text{Ti}_2\text{O}$
$\text{Na} + \text{TiS}_2 \rightarrow \text{NaTiS}_2$	$17\text{Na} + 17\text{TiS}_2 \rightarrow 7\text{TiS} + \text{Na}_3\text{Ti}_{10}\text{S}_{20} + 7\text{Na}_2\text{S}$
$\text{Na} + \text{TiSe}_2 \rightarrow \text{NaTiSe}_2$	$4\text{Na} + 4\text{TiSe}_2 \rightarrow \text{Na}_4\text{TiSe}_4 + \text{Ti}_3\text{Se}_4$
$\text{Na} + \text{VO}_2 \rightarrow \text{NaVO}_2$	$5\text{Na} + 5\text{VO}_2 \rightarrow \text{V} + \frac{1}{2}\text{Na}_5\text{V}_7\text{O}_{14} + \text{Na}_3\text{VO}_4$
$\text{Na} + \text{VS}_2 \rightarrow \text{NaVS}_2$	$3\text{Na} + 3\text{VS}_2 \rightarrow \text{V}_3\text{S}_4 + \frac{1}{2}\text{Na}_3\text{VS}_4 + \text{Na}_2\text{S}$
$\text{Na} + \text{VSe}_2 \rightarrow \text{NaVSe}_2$	$5\text{Na} + 5\text{VSe}_2 \rightarrow 2\text{Na}_2\text{Se} + \frac{1}{2}\text{Na}_3\text{V}_5\text{Se}_{10} + \text{V}_3\text{Se}_4$
$\text{Na} + \text{CrO}_2 \rightarrow \text{NaCrO}_2$	$12\text{Na} + 12\text{CrO}_2 \rightarrow 4\text{Cr}_2\text{O}_3 + 3\text{Na}_4\text{CrO}_4 + \text{Cr}$
$\text{Na} + \text{CrS}_2 \rightarrow \text{NaCrS}_2$	$2\text{Na} + 2\text{CrS}_2 \rightarrow \text{Cr}_2\text{S}_3 + \text{Na}_2\text{S}$
$\text{Na} + \text{CrSe}_2 \rightarrow \text{NaCrSe}_2$	$2\text{Na} + 2\text{CrSe}_2 \rightarrow \text{Na}_2\text{Se} + \text{Cr}_2\text{Se}_3$
$\text{Na} + \text{MnO}_2 \rightarrow \text{NaMnO}_2$	$5\text{Na} + 5\text{MnO}_2 \rightarrow \text{NaMn}_3\text{O}_4 + 2\text{Na}_2\text{MnO}_3$
$\text{Na} + \text{MnS}_2 \rightarrow \text{NaMnS}_2$	$6\text{Na} + 6\text{MnS}_2 \rightarrow \text{Na}_6\text{MnS}_4 + 3\text{MnS}_2 + 2\text{MnS}$
$\text{Na} + \text{MnSe}_2 \rightarrow \text{NaMnSe}_2$	$10\text{Na} + 10\text{MnSe}_2 \rightarrow 2\text{Na}_2\text{Mn}_2\text{Se}_3 + \text{Na}_6\text{MnSe}_4 + 5\text{MnSe}_2$
$\text{Na} + \text{FeO}_2 \rightarrow \text{NaFeO}_2$	$6\text{Na} + 6\text{FeO}_2 \rightarrow \text{Na}_3\text{Fe}_5\text{O}_9 + \frac{1}{2}\text{Na}_7\text{Fe}_3\text{O}_8$
$\text{Na} + \text{FeS}_2 \rightarrow \text{NaFeS}_2$	$2\text{Na} + 2\text{FeS}_2 \rightarrow \text{FeS}_2 + \text{FeS} + \text{Na}_2\text{S}$
$\text{Na} + \text{FeSe}_2 \rightarrow \text{NaFeSe}_2$	$2\text{Na} + 2\text{FeSe}_2 \rightarrow \text{Na}_2\text{Se} + \text{FeSe}_2 + \text{FeSe}$
$\text{Na} + \text{CoO}_2 \rightarrow \text{NaCoO}_2$	$6\text{Na} + 6\text{CoO}_2 \rightarrow \text{CoO} + \text{Na}_3\text{CoO}_3 + \text{Na}_3\text{Co}_4\text{O}_8$
$\text{Na} + \text{CoS}_2 \rightarrow \text{NaCoS}_2$	$4\text{Na} + 4\text{CoS}_2 \rightarrow \text{Co}_3\text{S}_4 + \text{CoS}_2 + 2\text{Na}_2\text{S}$
$\text{Na} + \text{CoSe}_2 \rightarrow \text{NaCoSe}_2$	$20\text{Na} + 20\text{CoSe}_2 \rightarrow \text{Co}_9\text{Se}_8 + 10\text{Na}_2\text{Se} + 11\text{CoSe}_2$
$\text{Na} + \text{NiO}_2 \rightarrow \text{NaNiO}_2$	$2\text{Na} + 2\text{NiO}_2 \rightarrow 0\text{Na}_{13}\text{Ni}_{11}\text{O}_{24} + 0\text{Na}_9\text{Ni}_{11}\text{O}_{20}$
$\text{Na} + \text{NiS}_2 \rightarrow \text{NaNiS}_2$	$4\text{Na} + 4\text{NiS}_2 \rightarrow \text{Ni}_3\text{S}_4 + \text{NiS}_2 + 2\text{Na}_2\text{S}$
$\text{Na} + \text{NiSe}_2 \rightarrow \text{NaNiSe}_2$	$4\text{Na} + 4\text{NiSe}_2 \rightarrow \text{NiSe}_2 + 2\text{Na}_2\text{Se} + \text{Ni}_3\text{Se}_4$
$\text{Li} + \text{TiO}_2 \rightarrow \text{LiTiO}_2$	$7\text{Li} + 7\text{TiO}_2 \rightarrow \text{Li}_7\text{Ti}_5\text{O}_{12} + 2\text{TiO}$
$\text{Li} + \text{TiS}_2 \rightarrow \text{LiTiS}_2$	$2\text{Li} + 2\text{TiS}_2 \rightarrow \text{TiS} + \text{Li}_2\text{S} + \frac{1}{2}\text{LiTi}_3\text{S}_6$
$\text{Li} + \text{TiSe}_2 \rightarrow \text{LiTiSe}_2$	$4\text{Li} + 4\text{TiSe}_2 \rightarrow 2\text{Li}_2\text{Se} + \text{Ti}_3\text{Se}_4 + \frac{1}{2}\text{LiTi}_3\text{Se}_6$
$\text{Li} + \text{VO}_2 \rightarrow \text{LiVO}_2$	$20\text{Li} + 20\text{VO}_2 \rightarrow \frac{1}{2}\text{Li}_7\text{V}_5\text{O}_{12} + \text{Li}_{17}\text{V}_{16}\text{O}_{32} + \text{V}_2\text{O}_3$
$\text{Li} + \text{VS}_2 \rightarrow \text{LiVS}_2$	$3\text{Li} + 3\text{VS}_2 \rightarrow \text{Li}_2\text{S} + \frac{1}{2}\text{Li}_3\text{VS}_4 + \text{V}_3\text{S}_4$









#### S4. Polymorphs considered in the determination of one-electron reaction voltages

The accompanying supplementary file `structures_SI.xlsx` contains information about the polymorphs used as electrode structures for the purposes of calculating the voltages displayed in the main manuscript. Structural information for the one-electron reactions can be found in the *I-electron reactions* tab of the spreadsheet. The spreadsheet contains, for each combination of working ion, transition metal, and anion considered in this work, an ID and spacegroup for the following structures:

1. ID for the discharged structure used to calculate the LDP voltage (Column name: ID for LDP discharged structure)

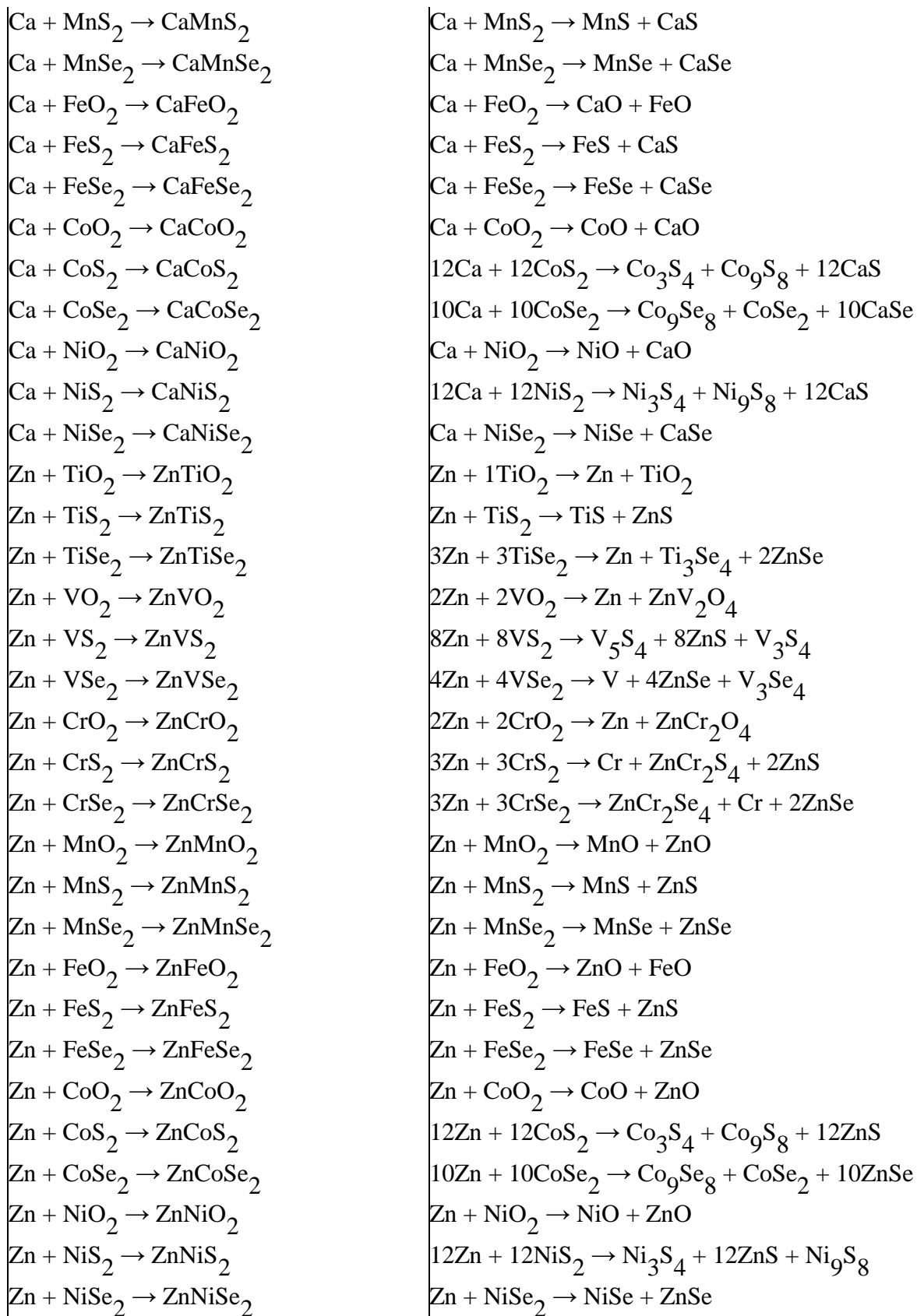
2. Spacegroup for the discharged structure used to calculate the LDP voltage (Column name: Spacegroup for LDP discharged structure)
3. ID for the charged structure to calculate the LCP voltage (Column name: ID for the LCP charged structure)
4. Spacegroup for the charged structure used to calculate the LCP voltage (Column name: Spacegroup for the LCP charged structure)
5. ID for the discharged structure used to calculate the LCP voltage (Column name: ID for the LCP discharged structure)
6. Spacegroup for the discharged structure used to calculate the LCP voltage (Column name: Spacegroup for the LCP discharged structure)

The ID fields contain either a Materials Project ID (an alphanumeric string beginning with "mp-" or "mvc-") or the stoichiometry of the compound. Any compound with a Materials Project ID can be accessed freely at <http://www.materialsproject.org>. Note that no ID is given for the charged structures used to calculate the LDP voltages; these structures in all cases were generated by removing the working ion from the stable discharged structure and re-relaxing the empty host according to the computational procedure described in the main manuscript. An asterisk (\*) in the ID cell on the spreadsheet indicates that a local calculation was used for that particular structure.

Some fields contain the phrase "Hypothetical structure" - in this case, a hypothetical structure exhibiting  $E^{\text{hull}}=100$  meV/atom was used, as described in the main manuscript.

## S5. Two-electron reactions considered in this work

Intercalation Reaction	Conversion Reaction
$\text{Mg} + \text{TiO}_2 \rightarrow \text{MgTiO}_2$	$\text{Mg} + \text{TiO}_2 \rightarrow \text{TiO} + \text{MgO}$
$\text{Mg} + \text{TiS}_2 \rightarrow \text{MgTiS}_2$	$\text{Mg} + \text{TiS}_2 \rightarrow \text{TiS} + \text{MgS}$
$\text{Mg} + \text{TiSe}_2 \rightarrow \text{MgTiSe}_2$	$8\text{Mg} + 8\text{TiSe}_2 \rightarrow \text{Ti}_3\text{Se}_4 + \text{Ti}_5\text{Se}_4 + 8\text{MgSe}$
$\text{Mg} + \text{VO}_2 \rightarrow \text{MgVO}_2$	$3\text{Mg} + 3\text{VO}_2 \rightarrow \text{V} + \text{MgV}_2\text{O}_4 + 2\text{MgO}$
$\text{Mg} + \text{VS}_2 \rightarrow \text{MgVS}_2$	$8\text{Mg} + 8\text{VS}_2 \rightarrow \text{V}_5\text{S}_4 + 8\text{MgS} + \text{V}_3\text{S}_4$
$\text{Mg} + \text{VSe}_2 \rightarrow \text{MgVSe}_2$	$4\text{Mg} + 4\text{VSe}_2 \rightarrow \text{V} + 4\text{MgSe} + \text{V}_3\text{Se}_4$
$\text{Mg} + \text{CrO}_2 \rightarrow \text{MgCrO}_2$	$3\text{Mg} + 3\text{CrO}_2 \rightarrow \text{Cr} + \text{MgCr}_2\text{O}_4 + 2\text{MgO}$
$\text{Mg} + \text{CrS}_2 \rightarrow \text{MgCrS}_2$	$4\text{Mg} + 4\text{CrS}_2 \rightarrow \text{Cr}_3\text{S}_4 + \text{Cr} + 4\text{MgS}$
$\text{Mg} + \text{CrSe}_2 \rightarrow \text{MgCrSe}_2$	$3\text{Mg} + 3\text{CrSe}_2 \rightarrow \text{Cr}_2\text{Se}_3 + \text{Cr} + 3\text{MgSe}$
$\text{Mg} + \text{MnO}_2 \rightarrow \text{MgMnO}_2$	$\text{Mg} + \text{MnO}_2 \rightarrow \text{MnO} + \text{MgO}$
$\text{Mg} + \text{MnS}_2 \rightarrow \text{MgMnS}_2$	$\text{Mg} + \text{MnS}_2 \rightarrow \text{MnS} + \text{MgS}$
$\text{Mg} + \text{MnSe}_2 \rightarrow \text{MgMnSe}_2$	$\text{Mg} + \text{MnSe}_2 \rightarrow \text{MnSe} + \text{MgSe}$
$\text{Mg} + \text{FeO}_2 \rightarrow \text{MgFeO}_2$	$\text{Mg} + \text{FeO}_2 \rightarrow \text{MgO} + \text{FeO}$
$\text{Mg} + \text{FeS}_2 \rightarrow \text{MgFeS}_2$	$\text{Mg} + \text{FeS}_2 \rightarrow \text{FeS} + \text{MgS}$
$\text{Mg} + \text{FeSe}_2 \rightarrow \text{MgFeSe}_2$	$\text{Mg} + \text{FeSe}_2 \rightarrow \text{FeSe} + \text{MgSe}$
$\text{Mg} + \text{CoO}_2 \rightarrow \text{MgCoO}_2$	$\text{Mg} + \text{CoO}_2 \rightarrow \text{CoO} + \text{MgO}$
$\text{Mg} + \text{CoS}_2 \rightarrow \text{MgCoS}_2$	$12\text{Mg} + 12\text{CoS}_2 \rightarrow \text{Co}_3\text{S}_4 + \text{Co}_9\text{S}_8 + 12\text{MgS}$
$\text{Mg} + \text{CoSe}_2 \rightarrow \text{MgCoSe}_2$	$10\text{Mg} + 10\text{CoSe}_2 \rightarrow \text{Co}_9\text{Se}_8 + \text{CoSe}_2 + 10\text{MgSe}$
$\text{Mg} + \text{NiO}_2 \rightarrow \text{MgNiO}_2$	$\text{Mg} + \text{NiO}_2 \rightarrow \text{NiO} + \text{MgO}$
$\text{Mg} + \text{NiS}_2 \rightarrow \text{MgNiS}_2$	$12\text{Mg} + 12\text{NiS}_2 \rightarrow \text{Ni}_3\text{S}_4 + \text{Ni}_9\text{S}_8 + 12\text{MgS}$
$\text{Mg} + \text{NiSe}_2 \rightarrow \text{MgNiSe}_2$	$\text{Mg} + \text{NiSe}_2 \rightarrow \text{NiSe} + \text{MgSe}$
$\text{Ca} + \text{TiO}_2 \rightarrow \text{CaTiO}_2$	$3\text{Ca} + 3\text{TiO}_2 \rightarrow \text{CaTiO}_3 + 2\text{CaO} + \text{Ti}_2\text{O}$
$\text{Ca} + \text{TiS}_2 \rightarrow \text{CaTiS}_2$	$\text{Ca} + \text{TiS}_2 \rightarrow \text{TiS} + \text{CaS}$
$\text{Ca} + \text{TiSe}_2 \rightarrow \text{CaTiSe}_2$	$8\text{Ca} + 8\text{TiSe}_2 \rightarrow \text{Ti}_3\text{Se}_4 + \text{Ti}_5\text{Se}_4 + 8\text{CaSe}$
$\text{Ca} + \text{VO}_2 \rightarrow \text{CaVO}_2$	$3\text{Ca} + 3\text{VO}_2 \rightarrow \text{V} + \text{CaV}_2\text{O}_4 + 2\text{CaO}$
$\text{Ca} + \text{VS}_2 \rightarrow \text{CaVS}_2$	$8\text{Ca} + 8\text{VS}_2 \rightarrow \text{V}_5\text{S}_4 + \text{V}_3\text{S}_4 + 8\text{CaS}$
$\text{Ca} + \text{VSe}_2 \rightarrow \text{CaVSe}_2$	$4\text{Ca} + 4\text{VSe}_2 \rightarrow \text{V} + \text{V}_3\text{Se}_4 + 4\text{CaSe}$
$\text{Ca} + \text{CrO}_2 \rightarrow \text{CaCrO}_2$	$3\text{Ca} + 3\text{CrO}_2 \rightarrow \text{CaCr}_2\text{O}_4 + \text{Cr} + 2\text{CaO}$
$\text{Ca} + \text{CrS}_2 \rightarrow \text{CaCrS}_2$	$4\text{Ca} + 4\text{CrS}_2 \rightarrow \text{Cr}_3\text{S}_4 + \text{Cr} + 4\text{CaS}$
$\text{Ca} + \text{CrSe}_2 \rightarrow \text{CaCrSe}_2$	$3\text{Ca} + 3\text{CrSe}_2 \rightarrow \text{Cr} + \text{Cr}_2\text{Se}_3 + 3\text{CaSe}$
$\text{Ca} + \text{MnO}_2 \rightarrow \text{CaMnO}_2$	$\text{Ca} + \text{MnO}_2 \rightarrow \text{MnO} + \text{CaO}$



### S6. Polymorphs considered in the determination of two-electron reaction voltages

The *2-electron reactions* tab of the supplementary spreadsheet `structure_SI.xlsx` contains information about which structures were considered in the calculation of voltages for two-electron reduction reactions presented in this work. The notations are the same as those described in Section S4.

### S7. Thermodynamic analysis of intercalation and conversion reactions in sulfides and selenides

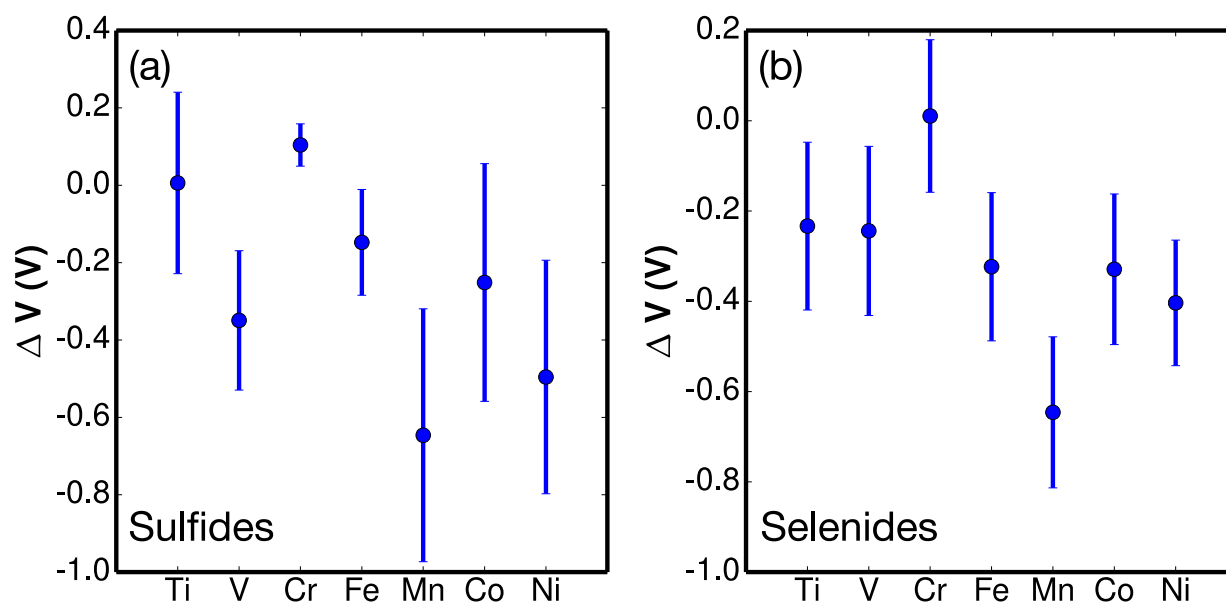


**Figure S3:** The difference between intercalation and conversion voltages for each transition metal

(a) sulfide and (b) selenide. Specifically,  $\Delta V = V_{\text{int}}^{\text{LDP}} - V_{\text{conv}}^{\text{LDP}}$ . The error bars represent the variation across possible working ions.

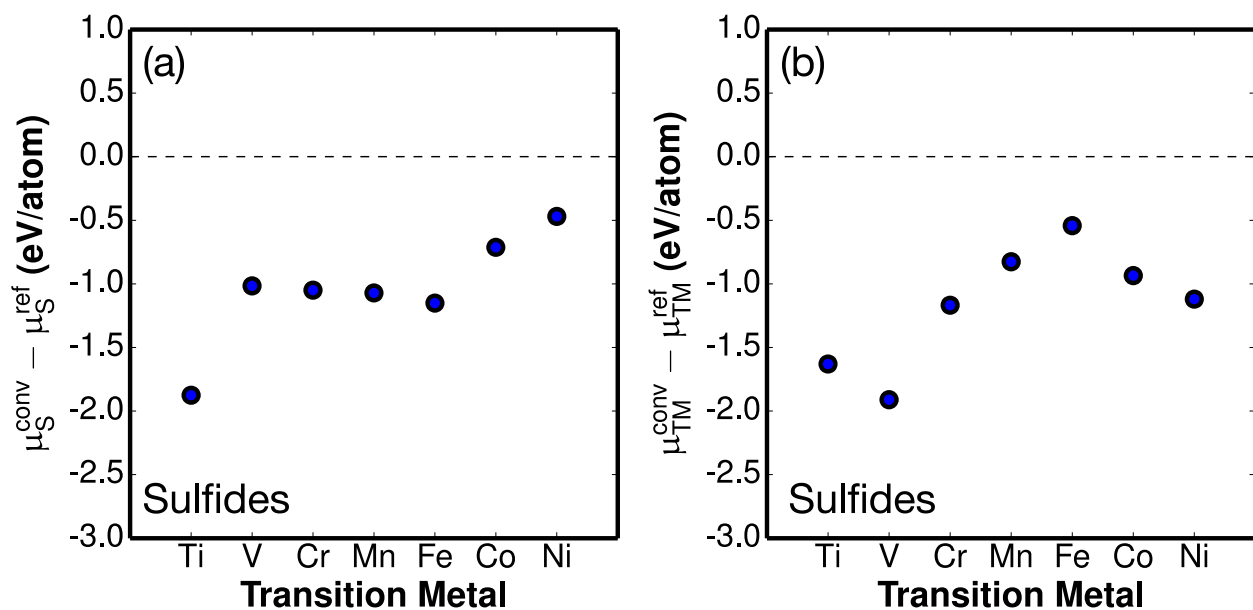


**Figure S4:** (a) and (b) show the referenced chemical potential set by the products of the conversion reaction for each particular transition metal sulfide. (a) displays the sulfide chemical potential, and (b) displays the transition metal chemical potential. In (a) and (b), we take the reference chemical potential to be the DFT energy of the bulk material.

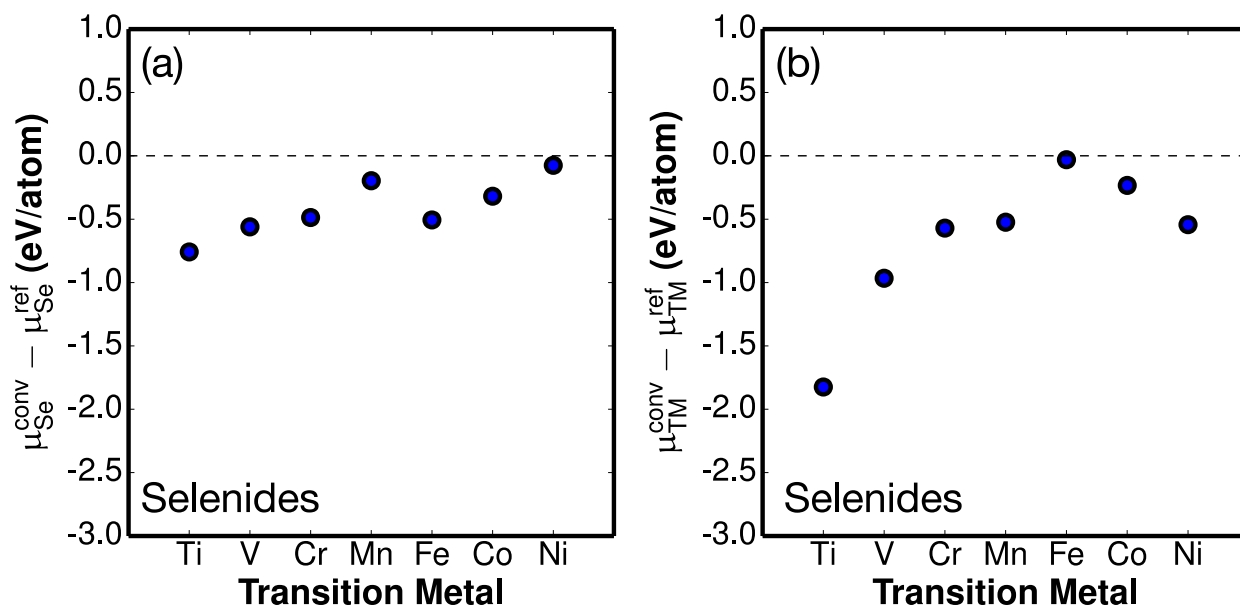


**Figure S5:** (a) and (b) show the referenced chemical potential set by the products of the conversion reaction for each particular transition metal selenide. (a) displays the selenide chemical potential, and (b) displays the transition metal chemical potential. In (a) and (b), we take the reference chemical potential to be the DFT energy of the bulk material.

### S7.1 Chemical potentials

To understand the thermodynamic underpinnings the competition between intercalation and conversion reactions, we can consider the reaction voltages (which are related to the free energy change of the reaction –  $\Delta G$  – via Eq. 1 in the main text) in terms of chemical potential changes. As an example, we analyze the balance of conversion and intercalation in  $\text{MgCr}_2\text{O}_4$ :



If we difference the intercalation and conversion reactions shown above we arrive at the (hypothetical) reaction  $\text{MgCr}_2\text{O}_4 \rightarrow \text{MgO} + \text{Cr}_2\text{O}_3$ , which does not evolve spontaneously if the  $\Delta G > 0$ . This is equivalent to stating that intercalation is the favored process if  $\Delta V > 0$ .  $\Delta G$  can in turn be described by Equation 1, wherein  $\mu_i$  indicates the chemical potential of species  $i$ .

$$\Delta G = \Delta\mu_{\text{Mg}} + \Delta\mu_{\text{Cr}} + \Delta\mu_{\text{O}} \quad (1)$$

Expanding each of the terms in Equation 1 yields Equation 2:

$$\Delta G = \left( \mu_{\text{Mg}}^{\text{MgO}} - \mu_{\text{Mg}}^{\text{MgCr}_2\text{O}_4} \right) + \left( 2\mu_{\text{Cr}}^{\text{Cr}_2\text{O}_3} - 2\mu_{\text{Cr}}^{\text{MgCr}_2\text{O}_4} \right) + \left( \mu_{\text{O}}^{\text{MgO}} + 3\mu_{\text{O}}^{\text{Cr}_2\text{O}_3} - 4\mu_{\text{O}}^{\text{MgCr}_2\text{O}_4} \right) \quad (2)$$

where for example,  $\mu_{\text{Mg}}^{\text{MgO}}$  represents the chemical potential of Mg within MgO. The oxygen chemical potential in MgO and  $\text{Cr}_2\text{O}_3$  that form upon conversion, i.e. the terms  $\mu_{\text{O}}^{\text{MgO}}$  and  $\mu_{\text{O}}^{\text{Cr}_2\text{O}_3}$  in Equation 2, are necessarily the same since the two conversion products, if they form, should be in equilibrium with each other. Henceforth, we will denote the oxygen chemical potential in conversion products as  $\mu_{\text{O}}^{\text{conv}}$ . Equation 2 then becomes:

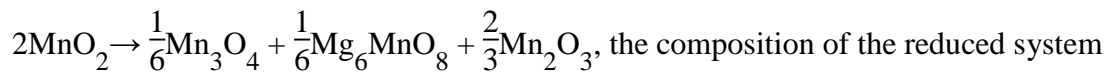
$$\Delta G = \left( \mu_{\text{Mg}}^{\text{MgO}} - \mu_{\text{Mg}}^{\text{MgCr}_2\text{O}_4} \right) + 2 \left( \mu_{\text{Cr}}^{\text{Cr}_2\text{O}_3} - \mu_{\text{Cr}}^{\text{MgCr}_2\text{O}_4} \right) + 4 \left( \mu_{\text{O}}^{\text{conv}} - \mu_{\text{O}}^{\text{MgCr}_2\text{O}_4} \right) \quad (3)$$



From Equation 3 it becomes clear that for a given reaction, higher chemical potentials in the conversion products will favor intercalation, i.e.  $\Delta G > 0$ . Further, only two out of the three chemical potentials are truly independent in Equation 3, owing to the Gibbs phase rule. To facilitate the analysis in a way that does not directly depend on the choice of the working ion, we consider  $\mu_{\text{TM}}$  and  $\mu_{\text{O}}$  as the independent chemical potentials.

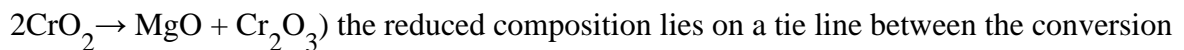
To examine how variation in the transition metal chemistry affects the chemical potential of the transition metal and oxygen in the conversion product equilibrium, we computed each chemical potential for the conversion reaction associated with each transition metal oxide. Note that two distinct definitions of the chemical potential arise:

1. When three products form as a result of the conversion reaction, as is the case in  $\text{Mg} +$



the composition of the reduced system ( $\text{Mg}+2\text{MnO}_2$ ) is bound by three phases on the ternary (Mg-Mn-O) phase diagram. In such scenarios, all three chemical potentials are uniquely defined by the free energies of the bounding phases.

2. When two products form as a result of the conversion reaction, (for example,  $\text{Mg} +$



the reduced composition lies on a tie line between the conversion products. In this case, we calculate the chemical potential of each species as the average of the triangular facets shared by the tie line ( $\text{MgO-Cr}_2\text{O}_3\text{-Cr}$  and  $\text{MgO-Cr}_2\text{O}_3\text{-MgCrO}_4$  in the Mg-Cr-O example).

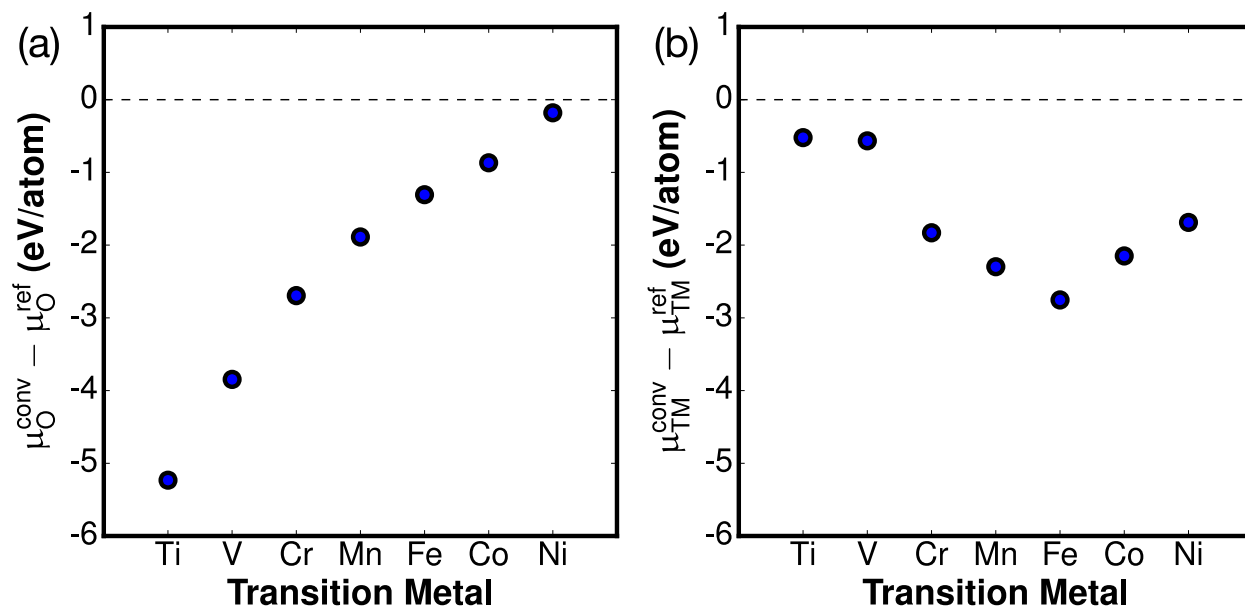


**Figure S6:** (a) and (b) show the referenced chemical potential set by the products of the conversion reaction for each particular transition metal. (a) displays the oxygen chemical potential, and (b) displays the transition metal chemical potential. In (b) and (c), we take the reference chemical potential to be the DFT energy of the bulk material.

Figures **Error! Reference source not found.**a and b display the variation of the oxygen and transition metal chemical potential, respectively, in the conversion products for several transition metals. In Figure **Error! Reference source not found.**, each chemical potential is referenced to the chemical potential of the corresponding element in its pure, bulk state  $\mu_{\text{TM}}^{\text{ref}}$ . The trends in Figures **Error! Reference source not found.**a and b exhibit different trends: The transition metal chemical potential tends to decrease initially across the  $3d$  period before increasing marginally for Co and Ni, while the oxygen chemical potential increases monotonically from Ti to Ni. The increase of oxygen chemical potential in the  $3d$ -oxides is consistent with the well-known decrease in oxygen affinity across the transition metal period.<sup>[1]</sup> The differing trends presented in Figure **Error! Reference source not found.** highlight an important optimization problem - some

transition metals, such as Ti, exhibit a high transition metal chemical potential which favors intercalation, but the oxygen chemical potential in Ti-oxides is low, favoring conversion. Evidently an optimal balance of these quantities is attained by Cr-oxides, which favor intercalation most strongly (Figure 6b in the main text).

### S8. $U$ values used in calculations

**Table S3:** To be compatible with the Materials Project database,<sup>[2]</sup> we used the following  $U$  values, only for oxides. Note that the pseudopotentials used in Materials Project are different from those used in the fit by Jain *et al.*,<sup>[3]</sup> resulting in different  $U$  values.

Transition metal	$U$ (eV)
Ti	–
V	3.25
Cr	3.7
Mn	3.9
Fe	5.3
Co	3.32
Ni	6.2

## References

- [1] K Kusabiraki, J Ikegami, T Nishimoto, T Ooka, *Oxidation of metals* **1997**, *47*, 411.
- [2] A. Jain, S. P. Ong, G. Hautier, W. Chen, W. D. Richards, S. Dacek, S. Cholia, D. Gunter, D. Skinner, G. Ceder, K. A. Persson, *APL Mat.* **2013**, *1*, 011002.
- [3] A. Jain, G. Hautier, S. P. Ong, C. J. Moore, C. C. Fischer, K. A. Persson, G. Ceder, *Phys. Rev. B* **2011**, *84*, 045115.